Published in final edited form as:

Nature. 2012 September 13; 489(7415): 304–308. doi:10.1038/nature11468.

Increased proteasome activity determines human embryonic stem cell identity

David Vilchez[1], **Leah Boyer**[2], **Ianessa Morantte**[1], **Margaret Lutz**[5], **Carsten Merkwirth**[1], **Derek Joyce**[1], **Brian Spencer**[3], **Lesley Page**[4], **Eliezer Masliah**[3], **W. Travis Berggren**[5], **Fred H. Gage**[2], and **Andrew Dillin**[1,*]

[1]Howard Hughes Medical Institute, Glenn Center for Aging Research, Molecular and Cell Biology Laboratory, The Salk Institute for Biological Studies, 10010 North Torrey Pines Road, La Jolla, CA 92037, USA

[2]Laboratory of Genetics, The Salk Institute for Biological Studies

[3]Department of Neurosciences, University of California, San Diego, 9500 Gilman Drive, La Jolla, CA 92093, USA

[4]Department of Cell Biology, The Scripps Research Institute, 10550 North Torrey Pines Road, La Jolla, CA 92037, USA

[5]Stem Cell Core, The Salk Institute for Biological Studies

Abstract

Embryonic stem cells are able to replicate continuously in the absence of senescence and, therefore, are immortal in culture[1,2]. While genome stability is central for survival of stem cells; proteome stability may play an equally important role in stem cell identity and function. Additionally, with the asymmetric divisions invoked by stem cells, the passage of damaged proteins to daughter cells could potentially destroy the resulting lineage of cells. We hypothesized that stem cells have an increased proteostasis ability compared to their differentiated counterparts and asked whether proteasome activity differed among human embryonic stem cells (hESCs). Notably, hESC populations exhibit a high proteasome activity that is correlated with increased levels of the 19S proteasome subunit PSMD11/RPN-6[3–5] and a corresponding increased assembly of the 26S/30S proteasome. Ectopic expression of PSMD11 is sufficient to increase proteasome assembly and activity. Proteasome inhibition affects pluripotency of hESCs inducing differentiation towards specific cell lineages. FOXO4, an insulin/IGF-1 responsive transcription factor associated with long lifespan in invertebrates[6,7], regulates proteasome activity by modulating the expression of PSMD11 in hESCs. Our results establish a novel regulation of

*Correspondence: Andrew Dillin, Molecular and Cell Biology Laboratory, The Salk Institute for Biological Studies, 10010 North Torrey Pines Road, La Jolla, CA 92037, USA, dillin@salk.edu.

AUTHOR CONTRIBUTIONS

D.V. and A.D. planned and supervised the project. D.V performed the experiments, data analysis and interpretation. L.B. performed neural differentiation assays, immunocytochemistry and contributed to other assays. I.M. performed biochemistry experiments and contributed to other assays. M.L. performed cell culturing and trophoblast/keratinocyte differentiation. C.M. performed biochemistry experiments and contributed to other assays. D.J. performed proteasome assembly experiments. B.S., L.P. and E.M. generated lentiviral constructs. W.T.B. and F.H.G. contributed with his knowledge of stem cell biology and neural differentiation and help to supervise the project. The manuscript was written by D.V. and A.D. and edited by L.B., I.M., C.M., W.T.B. and F.H.G. All authors discussed the results and commented on the manuscript.

proteostasis in hESCs that links longevity and stress resistance in invertebrates with hESC function and identity.

ESCs are unique among all stem cell populations examined insofar as they do not appear to undergo replicative senescence[1,2]. Since the ability to ensure proteostasis is critical for maintaining proper cell function[8,9], hESCs could provide a novel paradigm to define proteostasis regulation and its demise in aging. Central to proteostasis is the ubiquitin proteasome system and we hypothesized whether proteasome activity changes as hESCs differentiate into several cell lineages. To evaluate differences in the 26S/30S proteasome activity, we monitored the degradation of specific fluorogenic peptide substrates[10]. We differentiated H9 hESCs into neural progenitors cells (NPCs), which were then further differentiated into neurons. We found a dramatic decrease in the chymotrypsin-like proteasome activity when H9 hESCs were differentiated into NPCs (Fig. 1a). Moreover, when NPCs were differentiated into neurons, we detected a further decrease in proteasome activity that was observable after 2 weeks during the differentiation process (Fig. 1a and Supplementary Fig. 1). Consistent with enhanced proteasome activity in hESCs, we found increased levels of polyubiquitinylated proteins in differentiated cells compared to hESCs (Fig. 1b). Since hESCs are known to vary in their characteristics despite unlimited capacity of self-renewal[11], we differentiated a distinct hESC line, HUES-6 cells, and found similar results (Supplementary Fig. 1–2). Proteasome inhibitors blocked activity from extracts of hESCs, NPCs and neurons (Supplementary Fig. 3), indicating that indeed the increased peptidase activity was due to the proteasome. In addition, the other two activities of the proteasome, the caspase-like and trypsin-like, were also increased in hESCs (Fig. 1c–d). Proteasome activity did not differ depending on the passage number (Supplementary Fig. 4). The decrease in proteasome activity was not a specific phenomenon associated with the neural lineage since differentiation into either trophoblasts or fibroblasts induced a similar decrease (Fig. 1e–f). Notably, hESCs lost their high proteasome activity in a continuous progressive manner during the differentiation process (Fig. 1e). Moreover, we examined other cell lines extracted from human tissues, such as astrocytes or BJ fibroblasts, or immortalized HEK293T cell and found that these cells also had lower proteasome activity compared to hESCs (Supplementary Fig. 5). We tested whether high proteasome activity in hESCs was associated with increased proliferation and found that hESCs and HEK293T cells had nearly identical proliferation rates, yet hESCs had higher proteasome activity (Supplementary Fig. 6). Induced pluripotent stem cells (iPSCs) can be derived from adult somatic cells by forced expression of exogenous factors that promote cell reprogramming[12–14]. iPSC lines are similar to ESCs in many aspects, such as their gene expression patterns, proteome profile and potential for differentiation[13,15]. However, the full extent of their similarity to ESC is still being assessed[16]. We analyzed two iPSC lines carefully validated to ensure similar gene expression profile, growth characteristics and developmental potential to hESCs[17]. We discovered that these iPSC lines derived from BJ fibroblasts display increased proteasome activity similar to hESCs (Fig. 1g), indicating that proteasomal activity can indeed be reprogrammed.

The 26S/30S proteasome consists of a 20S core structure containing the proteolytic active sites and 19S cap structures that impart regulation on the activity of the holo-complex (26S,

single and 30S, double capped)[18]. Although 20S particles can exist in a free form, 20S particles in their most physiological form are inactive, unable to degrade denatured proteins or cleave peptides[10]. The 19S regulatory subunit is responsible for stimulating the 20S proteasome to degrade proteins, since ATPases of the regulatory particle open the 20S core, allowing substrates access to proteolytic active sites[19]. Treatment of cell extracts with 0.025% SDS, a condition that activates 20S particles by allowing gate opening[20], resulted in equivalent activities among all cell types (Fig. 2a and Supplementary Fig. 7). This result suggests that all cell types have an equal number of 20S particles, but hESCs have increased levels of active 26S/30S proteasomes. We examined the expression of the different 19S proteasome subunits and observed that PSMD11, the human orthologue of *rpn-6*, was the only 19S subunit to decrease as hESCs differentiated (Fig. 2b–g and Supplementary Fig. 8–10). Consistent with hESCs results, we observed increased PSMD11 levels in iPSCs (Fig. 2h–i). Accordingly, decreased expression of PSMD11 in hESCs (Supplementary Table 1) reduced proteasome activity (Fig. 2j), demonstrating that the increased levels of this subunit in hESCs are critical for increased proteasome activity. PSMD11 plays a critical role in stabilizing the otherwise weak interaction between the 20S core and the 19S cap[4], suggesting that hESCs might have more assembled proteasomes. We detected more 30S particles in hESCs compared to NPCs and neurons. Additionally, as more 20S subunits are assembled into 30S particles, less free 20S is found in hESCs (Fig. 2k). Ectopic expression of PSMD11 was sufficient to increase proteasome activity and assembly in cells with relatively low proteasome activity (Fig. 2l–m). Moreover, knockdown of PSMD11 resulted in fewer assembled proteasomes (Fig. 2n).

PSMD11/RPN-6 levels are increased in the long-lived *C. elegans glp-1* mutant. In this mutant, increased proteasome activity, *rpn-6* expression and longevity are modulated by the DAF-16/FOXO transcription factor. To examine whether FOXO transcription factors regulate proteasome activity in hESCs, we reduced expression of the closest human *daf-16* orthologues: FOXO1a, FOXO3a and FOXO4 (Supplementary Figure 11 and Supplementary Table 2). Strikingly, we found that FOXO4 was critical to modulate proteasome activity in hESCs whereas FOXO1a and FOXO3a, as well as a HSF-1, had little or no effect on proteasome activity (Fig. 3a–b and Supplementary Fig. 12). As hESCs differentiated into neural cells, trophoblasts or fibroblasts, FOXO4 had a corresponding decrease in its expression (Fig. 3c and Supplementary Fig. 13–15). Accordingly, this decrease in FOXO4 expression is reprogrammed from somatic cells to iPSCs (Fig. 3c). FOXO1a had a similar expression pattern to FOXO4 in H9 but not in HUES-6 hESCs (Supplementary Fig. 13–14). Furthermore, reduction of FOXO4 affected proteasome activity in the multipotent NPCs, which retain partial stem cell character, but did not affect proteasome activity in differentiated neurons (Supplementary Fig. 16 and Supplementary Table 3). These results raised the question whether FOXO4 regulation upon proteasome activity could be a general mechanism found in dividing cells. However, we found that FOXO4 was not required for proteasome activity regulation in BJ fibroblasts or HEK293T but rather appears specific to hESCs (Supplementary Fig. 17). FOXO4 transcriptional activity is inhibited by phosphorylation on Thr32, Ser197, and Ser262 sites and once dephosphorylated, it translocates to the nucleus and induces target gene expression[21,22]. Expression of constitutively active FOXO4 triple alanine mutant (FOXO4 AAA), but not wild-type

FOXO4, resulted in further up-regulation of proteasome activity in hESCs (Fig. 3d, Supplementary Fig. 18 and Supplementary Table 4a–b). In addition, ectopic expression of FOXO4 AAA in FOXO4 shRNA cells partially rescued the decreased proteasome activity of these cells (Fig. 3e and Supplementary Table 4c). We found that loss of FOXO4 resulted in reduced expression of PSMD11 in hESCs and in the multipotent NPCs, but did not affect PSMD11 in differentiated neurons (Fig. 3f–g and Supplementary Fig. 19). Knockdown of FOXO1a, FOXO3 or HSF-1 did not affect the expression of PSMD11 in any cell type tested, including hESCs (Supplementary Tables 5–7). Moreover, overexpression of FOXO4 AAA increased PSMD11 levels in hESCs (Fig. 3f–g and Supplementary Table 5). Ectopic expression of PSMD11 in FOXO4 shRNA hESCs rescued the decreased proteasome activity of these cells, indicating that expression of PSMD11 by FOXO4 is sufficient to regulate proteasome activity (Fig. 3g–h).

Prompted by these intriguing results, we tested whether FOXO4 was required for proper function of hESCs. We measured the expression levels of several markers of pluripotency in FOXO4 shRNA hESCs prior to differentiation and found no difference at this stage (Supplementary Table 8). However, when we forced differentiation into neural lineage (Supplementary Table 9), we observed that FOXO4 shRNA embryoid bodies had a diminished ability (65%–90% reduction) to generate rosettes and, accordingly, neural cells (Supplementary Fig. 20–24 and Supplementary Table 10). Ectopic expression of FOXO4 AAA partially restored the low ability of FOXO4 shRNA hESCs to differentiate into neural cells (Supplementary Fig. 24). On the contrary, ectopic expression of PSMD11 in FOXO4 shRNA hESCs was not sufficient to rescue this phenotype (Supplementary Fig. 25), indicating that FOXO4 has additional target genes that may be critical for neural differentiation. We asked whether differentiation into other cell lineages might also be affected by reduction of FOXO4 levels. Notably, after the respective differentiation process, FOXO4 shRNA hESCs were able to properly differentiate into either trophoblasts or keratinocytes and had increased levels of trophoblast or keratinocyte markers compared to control cells (Supplementary Fig. 26–27 and Supplementary Table 11). Taken together, our results suggest a role for FOXO4 in neural differentiation but the definitive role of FOXO4 in this process awaits future knockout experiments.

We tested whether PSMD11was required for neural differentiation. Due to the important role of PSMD11 in proteasomal function, an essential structure for the cell, we could not obtain stable hESCs with robust PSMD11 knockdown. However, even with weak reduction of PSMD11 we observed significant decreased expression of neural markers (β-III tubulin) in PSMD11 shRNA hESCs after neural differentiation. Although reduced β-III tubulin, these cells had a similar efficiency in the generation of embryoid bodies containing rosettes and/or neuronal projections (Supplementary Fig. 28). Because we could not achieve robust reduction of PSMD11, we induced an acute proteasome inhibition in hESCs by using MG-132 proteasome inhibitor to assess the requirement for proteasome activity in hESC function. Notably, hESCs were more sensitive to proteasome inhibition than NPCs or neurons and we had to decrease MG-132 concentration almost 100 times in order to avoid cell death and detachment of hESCs (data not shown). Strikingly, low concentrations of MG-132 (62.5 nM) were sufficient to reduce proteasome activity and induce accumulation of polyubiquitinylated proteins in hESCs (Supplementary Fig. 29). Even in the absence of

differentiation treatment, we already observed that proteasome inhibition resulted in decreased pluripotency markers and modified the levels of markers of the distinct germ and extraembryonic layers, while decreasing the expression of proteins involved in neurogenesis (Fig. 4). Taken together, these results suggest that acute proteasome inhibition affects pluripotency of hESCs inducing differentiation towards specific cell lineages to the detriment of neurogenesis.

Collectively, our results establish increased proteasome activity as an intrinsic characteristic of hESC identity. Our findings raise the intriguing question of why these cells need enhanced proteasome activity. One possibility is that hESC cannot tolerate toxic, misfolded proteins and increased proteostasis could be required to avoid hESC senescence and maintain an intact proteome either for self-renewal or the generation of an intact cell lineage. Alternatively, the high proteasome activity may be tightly linked to other cellular process, such as translation, to ensure future integrity of the proteome. In addition, our results indicate that an orthologue of DAF-16, a transcription factor that regulates both lifespan and resistance to proteotoxic stress in invertebrates, crosses evolutionary boundaries and links hESC function to invertebrate longevity modulation. It will be of particular interest to identify additional genes of the proteostasis network regulated by FOXO4 in hESCs. In conclusion, our findings may trigger new advances in understanding hESC differentiation or cell reprogramming and open new possibilities for cell therapy by modulation of the proteostasis network.

METHODS

hESCs culture and differentiation

Human H9 (WA09) hESC line was obtained from WiCell Research Institute. HUES-6 hESC line was obtained from the Laboratory of Douglas Melton, Harvard University. hESC lines were maintained on a mitotically inactive mouse embryonic fibroblast (MEFs) feeder layer in hES medium, DMEM/F12 (Invitrogen) supplemented with 20% Knockout Serum Replacement (Invitrogen), 1 mM L-glutamine, 0.1 mM non-essential amino acids, β-mercaptoethanol and 10ng/ml bFGF (Joint Protein Central, S. Korea). When co-culturing hESCs with MEFs was not possible due to interference with downstream assays H9 hESCs were also maintained on Matrigel (BD Biosciences) using mTeSR1 (Stem Cell Technologies). When cultured on Matrigel, HUES-6 cells were fed on conditioned medium harvested from cultured MEFSs. hESC colonies were passaged using a solution of collagenase (1 mg/ml) or dispase (2 mg/ml) and scraping the colonies with a glass pipette. For our experimental assays, we used H9 hESCs passage 40–45 and HUES-6 hESCs passage 30–35. The human iPSC lines (control BJ-iPSC lines) were derived and characterized as previously reported[17] and cultured similarly as described above for hESCs cells.

Neural differentiation was performed as follows. hESCs grown on inactivated MEFs were fed with N2/B27 medium (DMEM/F12-GlutaMAX (Invitrogen), 1x N2 (Invitrogen) 1x B27 -RA (Invitrogen)) for two days prior to being treated with collagenase type IV (1mg/ml in DMEM/F12) at 37°C for ~1 hour. Once colonies lifted off the plate, they were gently washed and then transferred to ultra-low attachment plates (Corning). Aggregates (embryoid

bodies –hEBs) were allowed to form and were grown in suspension for 1 week in N2/B27 medium with medium changes as needed, roughly every other day. The hEBs were then transferred onto polyornithine (PORN)/laminin-coated plates in N2/B27 medium with 1 μg ml^{-1} laminin (Invitrogen) where they were allowed to adhere and develop neural rosettes and projections. After 1 week, colonies were either picked for neural precursor cell (NPC) line, or scored on an Olympus SZX10 dissecting microscope for the presence of neural rosettes or projections, before being fixed or harvested for RNA. Picked colonies containing rosettes or projections are dissociated with TrypLE (Invitrogen) for 5 minutes at 37°C and plated onto PORN/laminin coated plates in NPC medium (DMEM/F12, N2/B27-RA (Invitrogen), 1 μg/ml laminin and 20 ng/ml FGF2). The resulting monolayer culture was grown at a high density and split 1:3 every week. For our experimental assays, we used NPCs passage 10–14.

For neuronal differentiation, NPCs were dissociated with TrypLE (Invitrogen) and plated into neuronal differentiation medium (DMEM/F12, N2/B27-RA (Invitrogen), 1μg/ml laminin, 20ng/ml BDNF (Peprotech), 20ng/ml GDNF (Peprotech), 1mM dibutyryl-cyclic AMP (Sigma), 200nM ascorbic acid (Sigma)) onto PORN/laminin-coated plates. For this study, cells were differentiated in 6-well plates, with approximately $2x10^5$ cells per 6-well. Cells were differentiated for 2–3 months, with weekly feeding of neuronal differentiation medium.

Differentiation to fibroblast cells involved the formation of embryoid bodies (EBs) as described above but cultured in EB medium (IMDM base medium supplemented with 15% FBS (Atlanta Biologicals), 0.1 mM non-essential amino acids, and 1% Glutamax (Invitrogen) and maintained on ultra-low attachment plates with daily medium changes. 1 week later the floating EBs were plated on gelatin-coated plates and passaged at confluence 3 times before use. Alternatively, a non-EB method was employed involving the individualization of hESCs using Accutase 1x (Millipore) and plating the cells at a density of $25x10^3$ cells per square cm in EB medium containing Rock Inhibitor (Y-27632, Stemgent) at 10μM. The cells were fed daily with straight EB medium. At confluence any areas still showing a stem cell morphology were removed by aspiration then passaged using Accutase 1x. After 3 passages the cells present with fibroblast morphology and were confirmed by PCR of lineage specific markers.

Trophoblast differentiation was performed as described previously using high levels of BMP4[23]. Keratinocyte differentiation was performed following the protocol established in[24]. BJ human fibroblasts (ATCC, CRL-2522) were cultured in DMEM (Invitrogen) supplemented with 10% FBS and 0.1 mM non-essential amino acids and passaged with trypsin. Hippocampal and Cerebellar Astrocytes are from Sciencell, Carlsbad, CA.

Generation of lentiviral vectors

The shRNA expressing lentiviral vectors were generated by cloning the sequences described in Supplementary Table 12 into the pSIH1-copGFP vector (SBI Biosystems, Mountain View, CA) to generate pLV-siHSF-1, pLV-siFOXO1a, pLV-siFOXO3a, pLV-siFOXO4, pLV-si3′UTR_1 FOXO4, pLV-si3′UTR_2 FOXO4 and pLV-si3′UTR_3 FOXO4. A control shRNA vector was generated by cloning the sequence CGT GCG TTG TTA GTA CTA ATC

CTA TTT designed against the sequence of luciferase (SBI Biosystems) into the same vector to generate pLV-siLuc. The GFP expressing vector was prepared from the 3rd generation self-inactivating lentivirus[25]. Lentiviruses were packaged by transient transfection in 293T cells[25].

LV-Non targeting shRNA Control, LV-shPSMD11_1 (Clone ID: TRCN0000003948), LV-shPSMD11_2 (TRCN0000003950), LV-shPSMC2_1(TRCN0000007181), LV-shPSMC2_2 (TRCN0000007183) in pLKO.1-puro-CMV-tGFP vector were obtained from Mission shRNA (Sigma).

FOXO4 overexpressing lentiviral constructs were generated as follows. Flag-FOXO4 construct was obtained from Addgene (plasmid 17549). PCR was performed to generate a product to be cloned into pLVX puro lentiviral plasmid (Clontech) utilizing the XhoI/SmaI sites.

Forward primer (with 5′ XhoI site for cloning):

CGC GTA CTC GAG ATG GAT CCG GGG AAT GAG AAT TCA GCC ACA GAG GCT GCC GCG ATC ATA GAC.

Reverse primer (with 3′ SmaI site for cloning);

CCG GAA CCC GGG TCA GGG ATC TGG CTC AAA G.

To generate FOXO4 AAA (Thr 32, Ser 197, Ser 262), site-directed mutagenesis of FOXO4 wild-type was performed by using Pfu Turbo. The primers used for site-directed mutagenesis were:

T32A(FW)	GTC CCC GCT CCT GTG CTT GGC CCC TTC C
T32A(RV)	GG AAG GGG CCA AGC ACA GGA GCG GGG AC
S197A(FW)	GCA AAG CCC CCC GCC GCA GAG CCG CAG CCA TGG ATA GCA GCA G
S197A(RV)	CTG CTG CTA TCC ATG GCT GCG GCT CTG CGG CGG GGG GCT TTG C
S262A(FW)	GTC CAC GAA GCA GCG CAA ATG CCA GCA GTG TCA GC
S262A(RV)	GCT GAC ACT GCT GGC ATT TGC GCT GCT TCG TGG AC

PCR was performed with one set of primers at a time. DpnI was added to the PCR product for 2hr/37°C before transformation of DH5a bacteria. Plasmid preps were sequenced before the next mutation introduced.

PSMD11 overexpressing lentiviral construct was generated as follows. Human PSMD11 cDNA was PCR amplified and cloned into pLVX-Puro using XhoI and BamHI. Resulting constructs were transformed into One Shot Stbl3 *E. coli* (Invitrogen). Constructs were sequence verified and thereafter transfected into packaging cells to produce high titer lentivirus.

Lentiviral infection of human stem cells

hESC colonies growing on Matrigel were incubated with mTesR1 medium containing 10 μM ROCK inhibitor (Y-27632) for one hour and individualized using Accutase 1x. $5x10^5$ cells were infected in suspension with 10 μl of concentrated lentivirus in the presence of 10

μM ROCK inhibitor. Cell suspension was centrifuged to remove virus, passed through a mesh of 40 μM to obtain individual cells and plated back on a feeder layer of fresh MEFs in hESC cell media supplemented with 10 μM ROCK inhibitor. After a few days in culture, small hES cell colonies arose. For LV-GFP and LV-shFOXOs stable lines, GFP positive colonies were selected and manually passaged onto fresh MEFs to establish new hESC cell lines. For LV-non-targeting shRNA, shPSMD11, shPSMC2, FOXO4 OE, FOXO4 AAA OE and PSMD11 OE stable lines, we performed 1 μg/ml puromycin resistance selection during 3 days and then colonies were manually passaged onto fresh MEFs to establish new hESC cell lines.

Transient infection experiments were performed as follows. hESC colonies growing on Matrigel were incubated with mTesR1 medium containing 10 μM ROCK inhibitor (Y-27632) for one hour and individualized using Accutase 1x. $1x10^5$ cells were plated on Matrigel plates and incubated with mTesR1 medium containing 10 μM ROCK inhibitor (Y-27632) for one day. Cells were infected with 2 μl of concentrated lentivirus. Plates were centrifuged at 800 rpm for 1 h at 30°C. Cells were fed with fresh media the day after to remove virus. NPCs were split as described above, and infected with 2 μl of concentrated lentivirus for 1 day. Neurons were infected after 2 months of differentiation with 2 μl of concentrated lentivirus for 1 day. In all the cases, cells were collected for experimental assays after 4 days of infection.

26S proteasome fluorogenic peptidase assays

In vitro assay of 26S proteasome activities was performed as previously described[10]. Cells were collected in proteasome activity assay buffer (50 mM Tris-HCl (pH 7.5), 250 mM sucrose, 5 mM $MgCl_2$, 0.5 mM EDTA, 2 mM ATP and 1 mM dithiothreitol) and lysed by passing 10 times through a 27 gauge needle attached to a 1 ml syringe. Lysate was centrifuged at 10,000g for 10 min at 4°C. 15–25 μg of total protein of cell lysates were transferred to a 96-well microtiter plate (BD Falcon) and then the fluorogenic substrate was added to lysates. For measuring the chymotrypsin-like activity of the proteasome we used either Z-Gly-Gly-Leu-AMC (Enzo) or Suc-Leu-Leu-Val-Tyr-AMC (Enzo). We used Z-Leu-Leu-Glu-AMC (Enzo) to measure the caspase-like activity of the proteasome and Ac-Arg-Leu-Arg-AMC for the proteasome trypsin-like activity. Fluorescence (380-nm excitation, 460-nm emission) was monitored on a microplate fluorometer (Infinite M1000, Tecan) every 5 min for 1 h at 37°C. Protein concentration of the cell homogenates was determined using the BCA protein assay (Pierce).

Native gel immunoblotting of the proteasome

hESCs (H9), NPCs and neurons were collected in proteasome activity assay buffer (50 mM Tris-HCl (pH 7.6), 5 mM $MgCl_2$, 0.5 mM EDTA, 5 mM ATP, 1 mM dithiothreitol and 10% glycerol supplemented with Roche phosphatase inhibitors) and lysed by passing 10 times through a 27 gauge needle attached to a 1 ml syringe. Lysate was centrifuged at 16,000g for 15 min at 4°C. 15μg of total protein was run on a 3–12% NativePAGE Bis-Tris gel (Invitrogen) in 1X NativePAGE running buffer (Invitrogen) at 4°C for 1 hour at 150V and then increased to 200V for a further hour. Proteins were then transferred to a PVDF membrane at 25V for 1 hour in 1X NativePAGE transfer buffer (Invitrogen) in an XCell II

Blot module (Invitrogen). Following transfer, the PVDF membrane was incubated for 20 min with 8% acetic acid to fix the proteins and dried. Western blot analysis was performed with anti-20S alpha 1–7 (Abcam) and anti-PSMD2 (Abcam).

HEK293T cells were run on 3.5% native gels prepared in resolving buffer (90 mM Tris base, 90mM boric acid, 5mM $MgCl_2$, 0.5mM EDTA, 1mM ATP) with 5 mM ATP, 1 mM dithiothreitol, and 3.5% acrylamide from a 40% stock solution of acrylamide and bisacrylamide in a 37.5:1 ratio (Bio-Rad, 161-0148). These were run at 110V for 3hr at 4°C. Activity assays were performed by incubating the gels in activity assay buffer for 20 min at 37°C and developed using a BioRad Gel Doc with UV illumination. Prior to transfer, the gels were incubated in transfer buffer (25 mM Tris base, 192 mM glycine) with 1% SDS for 10 min followed by a 10 min incubation in transfer buffer. The protein was transferred to PVDF at 5V for 16h in transfer buffer using an Idea Scientific Genie Blotter. Western blot analysis was performed with anti-PSMD1 (Abcam) and analyzed using the Odyssey system (LI-COR Biosciences). Extracts were also analyzed by SDS-PAGE to determine protein expression levels and loading control.

Western Blot

For analysis of proteasome subunits, cells were collected in proteasome activity assay buffer supplemented with protease inhibitors (Roche) and lysed by passing 10 times through a 27 gauge needle attached to a 1 ml syringe. Lysate was centrifuged at 10,000g for 10 min at 4°C. Protein concentration of the cell homogenates was determined using the BCA protein assay (Pierce). For analysis of transcription factor and polyubiquitinylated proteins, cells were harvested from tissue culture plates by cell scraping and lysed in protein cell lysis buffer (10 mM Tris-Cl pH7.4, 10 mM EDTA, 50 mM NaCl, 50 mM NaF, 1% Triton X-100, 0.1% SDS supplemented with 2 mM sodium orthovanadate, 1 mM PMSF and Complete Mini Protease and PhosSTOP inhibitor cocktail mix) for 2 hrs at 1,000 rpm and 4°C in a Thermomixer. Protein concentrations were determined with a standard Bradford protein assay (BioRad). 20–50 μg of total protein were separated by SDS-PAGE, transferred to nitrocellulose membranes (Whatman) and subjected to immunoblotting. Western blot analysis was performed with anti-FK1 (Enzo), anti-20S alpha 1–7 (Abcam), anti-Proteasome 20S C2 (Abcam), anti-Rpt6 (Biomol), anti-PSMD1 (Abcam), anti-PSMD2 (Abcam), anti-PSMD14 (Abcam), anti-PSMB6 (Abcam), anti-PSMD11 (Novus), anti-FoxO4 (55D4) (Cell Signaling), anti-FoxO1a (C29H4) (Cell Signaling), anti-SOX2 (D6D9) (Cell Signaling), anti-FGF5 (Abcam), anti-MSX1 (Abcam), anti-PAX6 (Abcam), anti-TIF1gamma (Abcam), anti-HERC2 (Abcam) and anti-β-actin (Abcam). The affinity of the antibody to PSMD11 has been characterized by detecting a decrease at the protein levels with shPSMD11 or an increase by ectopic expression of PSMD11. These experiments convincingly show differences in only one band and we ascribe any alteration of PSMD11 to this band.

Coomassie staining

Protein lysates were separated by SDS-PAGE and visualized directly in the gel by Coomassie staining[26]. Gels were incubated in fixing solution (50% methanol, 10% acetic acid, 100 mM ammonium acetate) for 60 min, stained with 0.025% Coomassie dye in 10%

acetic acid on a shaker overnight and destained twice in 10% acetic acid for 60 min. Gels were transferred to water and analyzed with the Odyssey imager (Li-Cor Bioscience).

Immunohistochemistry

Cells were fixed with paraformaldehyde (4% in PBS) for 15 minutes, followed by blocking and permeabilization (3% Donkey Serum, 0.1% Triton in PBS) for 30 minutes. Cells were incubated in primary antibody overnight at 4°C (Mouse anti Oct3/4, 1:200, Santa Cruz; Rabbit anti Tuj1, 1:400, Babco/Covance; Chicken anti-GFP, 1:400, Millipore), and in secondary for 2 hours at room temperature (1:250; DyLight 649 donkey anti rabbit, DyLight 549 donkey anti mouse, DyLight 488 donkey anti chicken IgY; Jackson Immuno Research). Cells were then stained with 0.5 μg ml^{-1} DAPI (4′,6-diamidino-2-phenylindole) and coverslipped with Vectashield. Images were acquired using either an Olympus IX51 fluorescent or a Bio-Rad confocal microscope.

Bromodeoxyuridine (BrdU) proliferation assay

Cells were incubated with media containing 10 mM BrdU for 40 minutes. Cells were fixed with formaldehyde 4% in PBS for 15 minutes and washed in PBS. Prior to permeabilization, cells were incubated for 1 hour in 2N HCl at room temperature followed by extensive washes in PBS. Cells were permeabilized with 0.5% Triton-X100 in PBS for 10 minutes and blocked with 5 % normal donkey serum in 1% PBS-BSA for 40 min at room temperature. Rabbit anti-BrdU antibody (ABD Serotech) was diluted in 1% PBS-BSA and used for overnight incubation followed by incubation with a biotinylated anti-rabbit secondary antibody (Vector) for additional 2 hours at room temperature. Finally, cells were incubated with streptavidin-AlexaFluor 568 (Jackson Immuno Research) for 1 hour. DAPI was used to visualize nuclei at a concentration of 0.5 μg ml^{-1} DAPI in PBS.

RNA isolation and quantitative RT–PCR

Total RNA was extracted using RNAbee (Tel-Test Inc). cDNA was created using the Quantitect Reverse Transcriptase kit (Qiagen). SybrGreen real-time qPCR experiments were performed as described in the manual using ABI Prism79000HT (Applied Biosystems) and cDNA at a 1:20 dilution. Data was analyzed with the comparative 2ΔΔCt method using β-actin and GAPDH as housekeeping genes. See Supplementary Table 13 for details about the primers used for this assay.

Supplementary Material

Refer to Web version on PubMed Central for supplementary material.

Acknowledgments

We thank Dr. William E. Balch for critical comments on this work. We thank Alexander Stauffer and Veronica Modesto for their help with BrdU assays and cell culture, respectively. We thank Chris Tse for his help with immunocytochemistry experiments. We thank Dr. Sergio Ruiz for advice on hESC culture and lentiviral infection. This work was supported by HHMI. David Vilchez was a recipient of the F.M. Kirby, Inc. Foundation Postdoctoral Scholar Award and Beatriu de Pinós (AGAUR) fellowship. F.H.G. acknowledges, Helmsley Foundation, JPB Foundation, Mathers Foundation, Lookout Fund and CIRM.

References

1. Evans MJ, Kaufman MH. Establishment in culture of pluripotential cells from mouse embryos. Nature. 1981; 292:154–156. [PubMed: 7242681]
2. Thomson JA, et al. Embryonic stem cell lines derived from human blastocysts. Science. 1998; 282:1145–1147. [PubMed: 9804556]
3. Isono E, Saito N, Kamata N, Saeki Y, Toh EA. Functional analysis of Rpn6p, a lid component of the 26 S proteasome, using temperature-sensitive rpn6 mutants of the yeast Saccharomyces cerevisiae. The Journal of biological chemistry. 2005; 280:6537–6547. [PubMed: 15611133]
4. Pathare GR, et al. The proteasomal subunit Rpn6 is a molecular clamp holding the core and regulatory subcomplexes together. Proceedings of the National Academy of Sciences of the United States of America. 2012; 109:149–154. [PubMed: 22187461]
5. Santamaria PG, Finley D, Ballesta JP, Remacha M. Rpn6p, a proteasome subunit from Saccharomyces cerevisiae, is essential for the assembly and activity of the 26 S proteasome. The Journal of biological chemistry. 2003; 278:6687–6695. [PubMed: 12486135]
6. Kenyon C, Chang J, Gensch E, Rudner A, Tabtiang R. A C. elegans mutant that lives twice as long as wild type. Nature. 1993; 366:461–464. [PubMed: 8247153]
7. Tatar M, et al. A mutant Drosophila insulin receptor homolog that extends life-span and impairs neuroendocrine function. Science. 2001; 292:107–110. [PubMed: 11292875]
8. Balch WE, Morimoto RI, Dillin A, Kelly JW. Adapting proteostasis for disease intervention. Science. 2008; 319:916–919. [PubMed: 18276881]
9. Powers ET, Morimoto RI, Dillin A, Kelly JW, Balch WE. Biological and chemical approaches to diseases of proteostasis deficiency. Annual review of biochemistry. 2009; 78:959–991.
10. Kisselev AF, Goldberg AL. Monitoring activity and inhibition of 26S proteasomes with fluorogenic peptide substrates. Methods in enzymology. 2005; 398:364–378. [PubMed: 16275343]
11. Osafune K, et al. Marked differences in differentiation propensity among human embryonic stem cell lines. Nature biotechnology. 2008; 26:313–315.
12. Takahashi K, et al. Induction of pluripotent stem cells from adult human fibroblasts by defined factors. Cell. 2007; 131:861–872. [PubMed: 18035408]
13. Takahashi K, Yamanaka S. Induction of pluripotent stem cells from mouse embryonic and adult fibroblast cultures by defined factors. Cell. 2006; 126:663–676. [PubMed: 16904174]
14. Yu J, et al. Induced pluripotent stem cell lines derived from human somatic cells. Science. 2007; 318:1917–1920. [PubMed: 18029452]
15. Hanna JH, Saha K, Jaenisch R. Pluripotency and cellular reprogramming: facts, hypotheses, unresolved issues. Cell. 2010; 143:508–525. [PubMed: 21074044]
16. Panopoulos AD, Ruiz S, Izpisua Belmonte JC. iPSCs: induced back to controversy. Cell Stem Cell. 2011; 8:347–348. [PubMed: 21474093]
17. Brennand KJ, et al. Modelling schizophrenia using human induced pluripotent stem cells. Nature. 2011; 473:221–225. [PubMed: 21490598]
18. Finley D. Recognition and processing of ubiquitin-protein conjugates by the proteasome. Annual review of biochemistry. 2009; 78:477–513.
19. Kohler A, et al. The axial channel of the proteasome core particle is gated by the Rpt2 ATPase and controls both substrate entry and product release. Molecular cell. 2001; 7:1143–1152. [PubMed: 11430818]
20. Coux O, Tanaka K, Goldberg AL. Structure and functions of the 20S and 26S proteasomes. Annual review of biochemistry. 1996; 65:801–847.
21. Kops GJ, et al. Direct control of the Forkhead transcription factor AFX by protein kinase B. Nature. 1999; 398:630–634. [PubMed: 10217147]
22. Matsuzaki H, Ichino A, Hayashi T, Yamamoto T, Kikkawa U. Regulation of intracellular localization and transcriptional activity of FOXO4 by protein kinase B through phosphorylation at the motif sites conserved among the FOXO family. J Biochem. 2005; 138:485–491. [PubMed: 16272144]

23. Xu RH, et al. BMP4 initiates human embryonic stem cell differentiation to trophoblast. Nature biotechnology. 2002; 20:1261–1264.

24. Itoh M, Kiuru M, Cairo MS, Christiano AM. Generation of keratinocytes from normal and recessive dystrophic epidermolysis bullosa-induced pluripotent stem cells. Proceedings of the National Academy of Sciences of the United States of America. 2011; 108:8797–8802. [PubMed: 21555586]

25. Tiscornia G, Singer O, Verma IM. Design and cloning of lentiviral vectors expressing small interfering RNAs. Nature protocols. 2006; 1:234–240. [PubMed: 17406238]

26. Schagger H. Tricine-SDS-PAGE. Nature protocols. 2006; 1:16–22. [PubMed: 17406207]

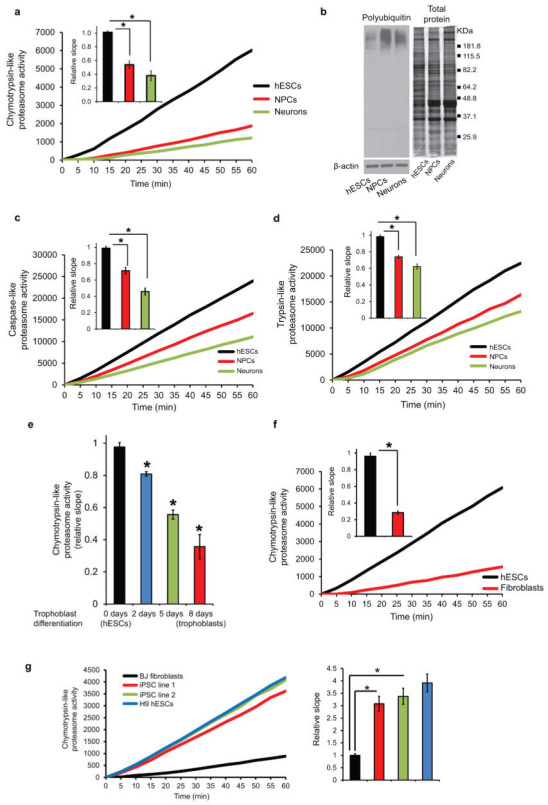

Figure 1. Increased proteasome activity in hESCs and iPSCs

a, Chymotrypsin-like proteasome activity measured fluorometrically by digestion of the peptide Z-GGL-AMC. Proteasome activity (relative slope to H9 hESCs) represents the mean ± s.e.m. (H9 hESCs (n=11), NPCs (n=13), neurons (n=10), (P<0.00001)). **b,** Representative immunoblot of polyubiquitinylated protein levels. β-actin loading control. Total protein was visualized by Coomassie staining in a corresponding protein gel. **c,** Caspase-like (Z-LLE-AMC) proteasome activity (relative slope to H9 hESCs) represents the mean ± s.e.m. (n=5, (P<0.001)). **d,** Trypsin-like (Ac-RLR-AMC) proteasome activity (relative slope to H9 hESCs) represents the mean ± s.e.m. (n=5, (P<0.0001)). **e,** Proteasome activity (relative slope to H9 hESCs) represents the mean ± s.e.m. (H9 hESCs (n=6), 2 days of differentiation into trophoblasts (n=6), 5 days of differentiation (n=6), trophoblasts (n=7)). H9 hESCs lose their high proteasome activity in a progressive manner when they differentiate into trophoblasts (H9 hESCs *vs* 2 days of differentiation into trophoblasts (P<0.001), H9 hESCs *vs* 5 days of differentiation ($P=7.7*10^{-7}$), H9 hESCs *vs* 8 days of differentiation (P<0.0001)). **f,** Proteasome activity (relative slope to H9 hESCs) represents the mean ± s.e.m. (n=3), (P<0.001). **g,** Chymotrypsin-like proteasome activity (relative slope to BJ fibroblasts) represents the mean ± s.e.m. (BJ fibroblasts (n=10), iPSC line 1 (n=10), iPSC line 2 (n=9), H9 hESCs (n=5)). iPSC lines derived from BJ fibroblast display increased proteasome activity compared to fibroblasts (P<0.0005) and no significant differences compared to H9 hESCs (iPSC line 1 *vs* H9 hESCs (P=0.11), iPSC line 2 *vs* H9 hESCs (P=0.29). Statistical comparisons in Figure 1 were made by Student's t-test for unpaired samples.

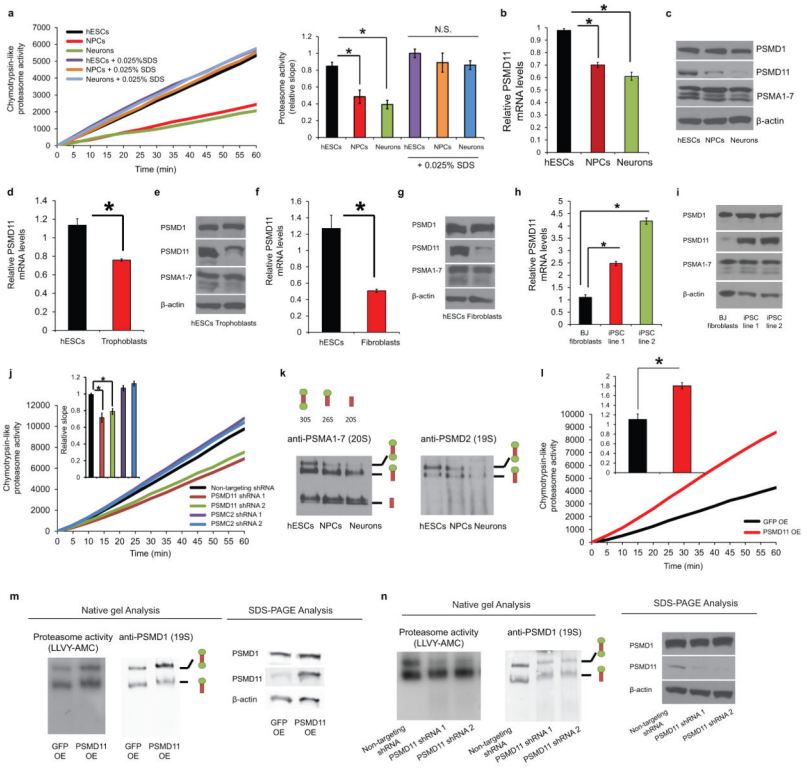

Figure 2. Increased proteasome assembly in hESCs dependent upon PSMD11 expression

a, Chymotrypsin-like proteasome activity (relative slope to H9 hESCs + 0.025% SDS) represents the mean ± s.e.m. (H9 hESCs (n=6), NPCs (n=5), neurons (n=5), H9 hESCs + 0.025% SDS (n=5), NPCs + 0.025% SDS (n=4), neurons + 0.025% SDS (n=5)). Increased proteasome activity in hESCs ($P<0.01$). No significant differences were found among the different cells when SDS was added (H9 hESCs + 0.025% SDS *vs* NPCs + 0.025% SDS ($P=0.25$), H9 hESCs + 0.025% SDS *vs* neurons + 0.025% SDS ($P=0.09$)). 0.025% SDS was added to cell lysates 5 minutes prior to digestion assay. **b,** Graph (relative expression to H9 hESCs) represents the mean ± s.e.m. (H9 hESCs (n=10), NPCs (n=6), neurons (n=8), ($P<0.00001$)). **c,** Western blot analysis with antibodies to PSMD11 and PSMD1. β-actin loading control. **d,** Graph (relative expression to H9 hESCs) represents the mean ± s.e.m. (n=4, ($P<0.05$). **e,** Western blot analysis of PSMD11 in trophoblasts. β-actin loading control. **f,** Graph (relative expression to H9 hESCs) represents the mean ± s.e.m. (n=4, ($P<0.05$)). **g,** Western blot analysis of PSMD11 in fibroblasts. β-actin loading control. **h,** Graph (relative expression to BJ fibroblasts) represents the mean ± s.e.m. (BJ fibroblasts (n=10), iPSC line 1 (n=6), iPSC line 2 (n=6), ($P<0.00001$)). **i,** Western blot analysis of PSMD11 in iPSC lines. β-actin loading control. **j,** Proteasome activity (relative slope to LV-Non-targeting shRNA) represents the mean ± s.e.m. (Non-targeting shRNA (n=10), PSMD11 shRNA 1 (n=8), PSMD11 shRNA 2 (n=6), PSMC2 shRNA 1 (n=6), PSMC2 shRNA 2 (n=3), ($P<0.01$)). **k,** Native gel electrophoresis followed by western blot with alpha 1+2+3+5+6+7 (20S subunit) or PSMD2 (19S subunit) antibodies. **l,** Chymotrypsin-like proteasome activity (relative slope to GFP OE HEK293T cells) represents the mean ± s.e.m. (GFP OE (n=4), PSMD11 OE (n=5), ($P<0.005$)). **m, n,** Native gel electrophoresis followed by proteasome activity assay

with chymotrypsin-like activity substrate LLVY-AMC and immunoblotting with PSMD1 (19S subunit) antibody. Extracts were resolved by SDS-PAGE and immunoblotting for analysis of PSMD11 levels and loading control. Statistical comparisons in Figure 2 were made by Student's t-test for unpaired samples.

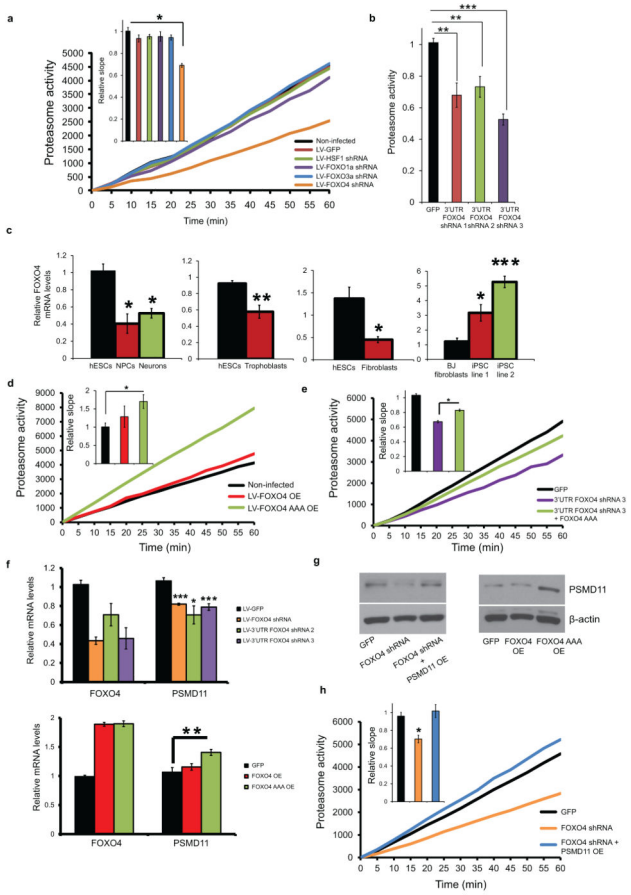

Figure 3. FOXO4 regulates proteasome activity in hESCs

a, Chymotrypsin-like proteasome activity in H9 hESCs transiently infected with lentiviruses (relative slope to non-infected cells) represents the mean ± s.e.m. (n=19, (P<0.00001)). **b,** Chymotrypsin-like proteasome activity (relative slope to GFP cells) represents the mean ± s.e.m. (GFP (n=7), 3′UTR FOXO4 shRNA 1(n=6), 3′UTR FOXO4 shRNA 2 (n=3), 3′UTR FOXO4 shRNA 3 (n=6)). Knockdown of FOXO4 decreases proteasome activity in stable infected H9 hESCs (GFP *vs* 3′UTR FOXO4 shRNA 1 (P<0.01), GFP *vs* 3′UTR FOXO4 shRNA 2(P<0.01), GFP *vs* 3′UTR FOXO4 shRNA 3 ($P=4.5*10^{-8}$)). **c,** FOXO4 levels are down-regulated when H9 hESCs differentiate into NPCs, neurons ((H9 hESCs (n=6), NPCs (n=4), neurons (n=4)), trophoblasts (H9 hESCs (n=6), trophoblasts (n=6)) and fibroblasts (H9 hESCs (n=4), fibroblasts (n=4)). No significant differences were found between NPCs and neurons (P=0.43). Graphs represent the mean ± s.e.m. of the relative expression levels to H9 hESCs. FOXO4 levels are up-regulated when BJ fibroblasts are reprogrammed into iPSCs (graph represents the mean ± s.e.m. of the relative expression levels to BJ fibroblasts (BJ fibroblasts (n=8), iPSC line 1 (n=6), iPSC line 2 (n=6)). *(P<0.05), **(P<0.01), ***(P<0.001). **d,** Proteasome activity (relative slope to non-infected H9 hESCs) represents the mean ± s.e.m. (n=7). Transient overexpression of FOXO4 AAA up-regulates chymotrypsin-like proteasome activity in H9 hESCs (non-infected cells *vs* LV-FOXO4 OE cells (P=0.41), non-infected cells *vs* LV-FOXO4 AAA OE cells (P<0.05)). **e,** Proteasome activity (relative slope to GFP hESCs) represents the mean ± s.e.m. (n=4, 3′UTR FOXO4

shRNA 3 *vs* 3′UTR_3 FOXO4 shRNA + FOXO4 AAA (P<0.01)). **f,** Knockdown of FOXO4 decreases expression of PSMD11 in H9 hESCs (GFP *vs* FOXO4 shRNA (P<0.001), GFP *vs* 3′UTR FOXO4 shRNA 2 (P<0.05), GFP *vs* 3′UTR FOXO4 shRNA 3 (P<0.001)). Graph represents the mean ± s.e.m (LV-GFP (n=15), LV-FOXO4 shRNA (n=19), LV-3′UTR FOXO4 shRNA 2 (n=4), LV-3′UTR FOXO4 shRNA 3(n=5)). Stable overexpression of FOXO4 AAA mutant increases PSMD11 expression in H9 hESCs (P=0.69 GFP *vs* FOXO4 OE, P<0.01 GFP *vs* FOXO4 AAA OE). Data represent the mean ± s.e.m. of the relative expression levels to GFP hESCs (GFP (n=7), FOXO4 OE (n=8), FOXO4 AAA OE (n=7)). **g,** Western blot analysis of PSMD11 levels. β-actin loading control. **h,** Proteasome activity (relative slope to GFP H9 hESCs) represents the mean ± s.e.m. (n=4, GFP *vs* FOXO4 shRNA (P<0.01), GFP *vs* FOXO4 shRNA+ PSMD11 OE (P=0.50)). Statistical comparisons in Figure 3 were made by Student's t-test for unpaired samples.

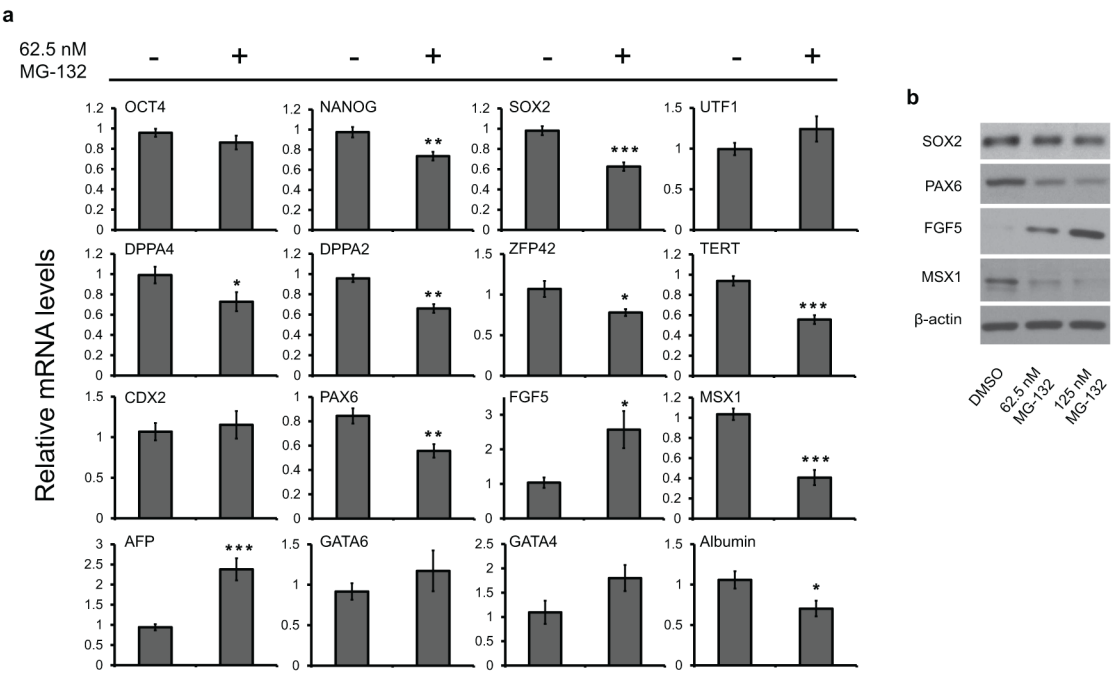

Figure 4. Acute proteasome inhibition affects pluripotency of hESCs

a, Real Time PCR analysis of pluripotency (OCT4, NANOG, SOX2, UTF1, DPPA4, DPPA2, ZFP42 and TERT), trophectodermal (CDX2), ectodermal (PAX6, FGF5), mesodermal (MSX1) and endodermal (AFP, GATA6, GATA4, Albumin) germ layer markers. Proteasome inhibition (62.5 nM MG-132 24h) in H9 hESCs induces a decrease in pluripotency markers and modified the levels of markers of the distinct germ cell and extraembryonic layers P-value: *(P<0.05), **(P<0.01), ***(P<0.001). Graph (relative expression to DMSO control H9 hESCs) represents the mean ± s.e.m. (DMSO (n=12), MG-132 (n=13). Statistical comparisons in Figure 4 were made by Student's t-test for unpaired samples. **b,** Western blot analysis with antibodies to SOX2, PAX6, FGF5 and MSX1. β-actin loading control.